Single channel in-line multimodal digital holography

Yair Rivenson,[1†,*] Barak Katz,[†] Roy Kelner, and Joseph Rosen

Department of Electrical and Computer Engineering, Ben-Gurion University of the Negev, P.O. Box 653, Beer-Sheva 8410501, Israel
**Corresponding author: rivenson@post.bgu.ac.il*

Received August 19, 2013; revised September 30, 2013; accepted October 9, 2013;
posted October 9, 2013 (Doc. ID 196030); published November 12, 2013

We present a new single channel in-line setup for holographic recording that can properly record various objects that cannot be recorded by the Gabor holographic method. This configuration allows the recording of holograms based on several modalities while addressing important issues of the original Gabor setup, including the well-known twin-image problem and the weak scattering condition.

OCIS codes: (090.0090) Holography; (090.1995) Digital holography; (110.6880) Three-dimensional image acquisition; (100.3010) Image reconstruction techniques; (070.6120) Spatial light modulators.
http://dx.doi.org/10.1364/OL.38.004719

Digital holography concerns the recording of a hologram using a solid-state detector array and the numerical reconstruction of the recorded object, or scene. Using a computer, the reconstruction is achieved via the decoding of the recorded hologram. Many methods of digital holography have been proposed throughout the years [1]. However, since the introduction of holography by Gabor [2], a single channel configuration has remained the most appealing type of hologram recording setup. In a single channel (in-line) holographic setup, the object and all other components are positioned on the same optical axis, enabling the use of low spatial and temporal coherence illumination sources and reduced stability requirements (see, e.g., [3]). Furthermore, maximal space-bandwidth-product can potentially be achieved [4]. In this Letter, we propose a new, to the best of our knowledge, single channel interferometer for the recording of digital holograms. This configuration can be described using the original Gabor holographic configuration [2]. Gabor originally described an in-line configuration, where the interference occurs between two wavefronts: one, scattered by the object, and another, which is unscattered. This principle imposes several restrictions on the object, such as the weak scattering condition. Under this condition, a large enough portion of the light must be unscattered upon passing through the object, so that it can be used as a reference wavefront; thus, making the Gabor setup impractical for dense samples. Another element that sets limits on the performance of the original Gabor holography is the twin image term, evident in the reconstruction. Throughout the years, several techniques have been proposed to remedy these problems. For example, computational techniques were suggested to remove the twin image [5] and bias terms [6]. Other methods have implemented optical and digital means that together perform an in-line phase-shifting technique. This was demonstrated for both incoherent [3,7] and coherent systems [8].

We propose a method by which the in-line hologram is formed through an interference of object scattered wavefront and unscattered wavefront, in a similar fashion to the original Gabor holography. However, the proposed method is superior to the Gabor working principle in the following manners: (1) Control over the reference field to object field intensity ratio is offered; that is, this ratio is no longer simply object dependent, remedying the weak scattering condition; (2) The complex field amplitude of the object can be extracted, either from a phase-shifting holography experiment or from a single shot, in the same manner as in off-axis holography. The twin-image problem is thus addressed; (3) The method allows the recording of Fresnel, image and (potentially) Fourier holograms, with only minor modifications to the setup, some of which are digitally set, without any mechanical movement of the equipment; and (4) The setup potentially can be used to perform on-axis reflection holography.

A schematic sketch of the recording setup is shown in Fig. 1. The setup contains two polarization dependent spatial light modulators (SLMs) located between two, in parallel polarizers, and a digital camera. The SLMs are placed with their active axes perpendicular to each other and at a 45° angle to the transmission axis of the two polarizers. The second polarizer is used to isolate, from the two orthogonal polarizations, two polarization components that have the same polarization direction and can, therefore, interfere [9]. As the input object is illuminated with a collimated laser beam, each SLM only phase-modulates components of the incident light

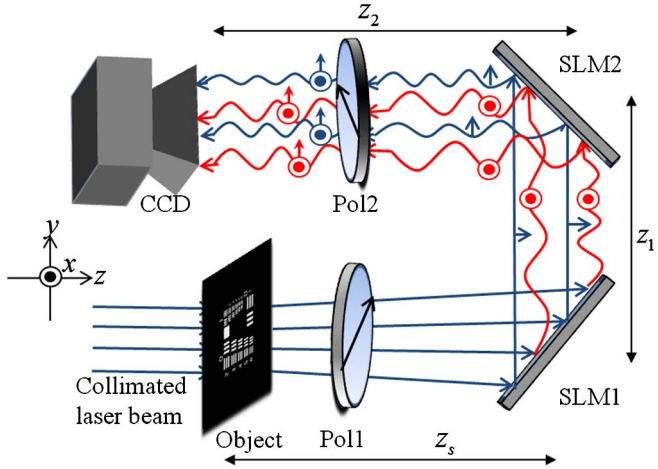

Fig. 1. Schematic of the JORDI recording setup. Pol1 and Pol2 are polarizers. The spatial light modulators are SLM1 and SLM2. The two independent beams are signified by red and blue. This is only a simplified scheme in the sense that the actual incident angles of the beams hitting the SLMs in the experimental setup are less than 10°.

that have their polarization aligned with its active axis, while components of perpendicular polarization, aligned with the nonactive axis of the SLM, are not affected [9]. This configuration enables separate control over perpendicular polarization components of the light beam traveling within the system. We coin our setup joint object reference digital interferometer (JORDI).

Let us denote the complex field amplitude of an object located inside a plane at a distance z_s away from the first SLM as $U(x,y;z_s)$. This wavefront propagates to the first SLM, where, due to the first polarizer, it is split into a modulated beam and unmodulated beam. The first beam, B_1, is used as the reference wavefront modulated by a converging lens function displayed on the SLM, such that the wavefront impinging on the CCD is:

$$B_1 = C_{\theta_1} U(x,y;z_s) * Q\left(\frac{1}{z_s}\right) \cdot Q\left(\frac{-1}{f_1}\right) L\left[\frac{\vec{a}_1}{f_1}\right] e^{j\phi_l} * Q\left(\frac{1}{z_1+z_2}\right), \quad (1)$$

where z_1, z_2, and z_s are the distances indicated on Fig. 1, f_1 is the focal length of the diffractive lens displayed on the first SLM, $Q(s) = \exp\{j\pi s\lambda^{-1}(x^2+y^2)\}$ is a quadratic phase term, $L[\vec{s}] = \exp\{j2\pi\lambda^{-1}(s_x x + s_y y)\}$ is a linear phase term, C_{θ_1} is a constant which accounts for the propagation constants and for the second polarizer angle with respect to the first SLM, and $\exp\{j\phi_l\}$ is a constant phase, used whenever a phase-shifting procedure is in order [3]. While the role of the $Q(s)$ function is to promote lens-like behavior, the role of the $L[\vec{s}]$ function is to introduce a tilt to the beam. The second beam, representing the part of the wavefront that was unmodulated by the first SLM, is modulated by the second SLM, which has its polarization axis positioned perpendicular to that of the first SLM. The second SLM also has a lens function displayed. The resulting wavefront of the second beam that impinges on the CCD is given by:

$$B_2 = C_{\theta_2} U(x,y;z_s) * Q\left(\frac{1}{z_s+z_1}\right) \cdot Q\left(\frac{-1}{f_2}\right) L\left[\frac{\vec{a}_2}{f_2}\right] * Q\left(\frac{1}{z_2}\right), \quad (2)$$

where f_2 is the focal length of the diffractive lens displayed on the second SLM, and C_{θ_2} accounts for propagation and for the exit polarizer angle, such that $\theta_2 = 90° - \theta_1$.

According to Eq. (1), whenever the function displayed on the first SLM, $Q(-1/f_1)$, is chosen such that $1/f_1 = 1/z_s + 1/(z_1+z_2)$, a shifted magnified image of the input object is formed on the CCD plane. Thus, the beam B_1 represents a reference beam that originates from the collimated laser beam plane wave, and is practically unscattered by the object. Therefore, upon reaching the CCD, assuming infinite extended apertures, it can be evaluated as $\tilde{C}_{\theta_1} Q\{1/(z_1+z_2-f_1)\} L\{-\vec{a}_1/(z_1+z_2-f_1)\}$ [10], where $\tilde{C}_{\theta_1}$ accounts for the constant phase terms and for C_{θ_1}. Therefore, this reference wave carries no information about the object in a similar fashion to the undiffracted wavefront that is used as a reference beam in Gabor holography. The main difference is that here the beam does not rely on the entire object distribution; rather, it uses just a magnified patch of the field of view that is unscattered by the object. This is schematically illustrated in Fig. 2, where the reference beam is marked in red. Thus, the resulting interference on the CCD is given by:

$$I \simeq \left| \tilde{C}_{\theta_1} Q\left(\frac{1}{z_1+z_2-f_1}\right) L\left(\frac{-\vec{a}_1}{z_1+z_2-f_1}\right) e^{j\phi_l} + B_2 \right|^2. \quad (3)$$

To demonstrate some of the various capabilities of JORDI, experimental results from several configurations are presented. The first experiment demonstrates the recording of a phase-shifting Fresnel hologram of a three-dimensional object. The input object was composed from two resolution charts, separated 10 cm apart from each other (depth-wise), and illuminated with a collimated He–Ne laser with central wavelength of $\lambda = 632$ nm. The front resolution chart was placed at $z_s = 35$ cm from the first SLM (Holoeye PLUTO, 1920 × 1080 pixels, 8 μm pixel pitch, with phase-only modulation). The other distances were set as follows: $z_1 = 28$ cm and $z_2 = 20$ cm. To create an image of the collimated, unscattered by the object, wavefront on the CCD plane (PixelFly CCD, 1280 × 1024 pixels, 6.7 μm pixel pitch, monochrome), the converging diffractive lens function on the first SLM was set to a focal length $f_1 = 20$ cm. The second diffractive lens focal length was set to $f_2 = 14$ cm to create a Fresnel hologram of the object. Three holograms were recorded with $\phi_l = \{0°, 120°, 240°\}$ and using the phase-shifting method [3] to eliminate the bias (zero-order) and twin-image terms. Following the recording, the complex field

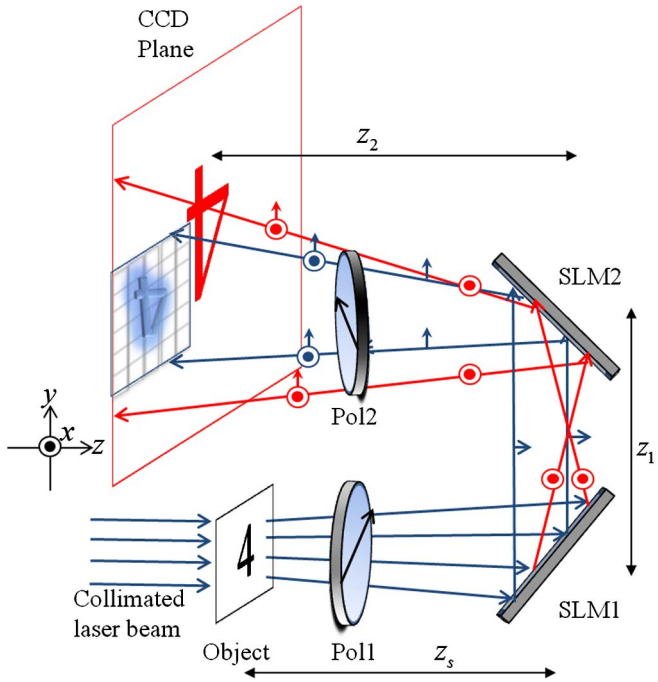

Fig. 2. Schematic of the hologram recorder implemented using the JORDI configuration. The reference beam, which is unscattered by the object (red arrows), interferes with the object wavefront (blue arrows) on the CCD.

amplitude of the object was extracted. A recorded hologram with $\phi_l = 0°$ is shown in Fig. 3(a), while the magnitude and phase of the resulting hologram, after applying the phase-shifting procedure, are shown in Figs. 3(b) and 3(c), respectively. Numerical refocusing on two of the object planes, using the Fresnel back-propagation procedure, is shown in Figs. 3(d) and 3(e).

In the second experiment, we demonstrate the capability of JORDI to record an image hologram. In this configuration, the first beam is being used as a reference wavefront, as in the previous experiment. The second beam is modulated by the second SLM using the function $Q(-1/f_2)$, such that $1/f_2 = 1/(z_s + z_1) + 1/z_2$. Thus, the second beam forms a magnified wavefront of the object on the CCD plane, such that the recorded interference can be approximated by:

$$I \simeq \left| \tilde{C}_{\theta_1} Q\left(\frac{1}{z_1 + z_2 - f_1}\right) L\left(\frac{-\vec{a}_1}{z_1 + z_2 - f_1}\right) e^{j\theta_l} + \frac{C_{\theta_2}}{|M|} U(x/M, y/M; z_s) \right|^2, \quad (4)$$

where M is the transverse magnification of the second imaging system. For reduced notation, it is assumed in Eq. (4) that the dimensions of the image are small enough to neglect the quadratic phase term that multiplies the image term $U(\bullet)$ [11]. However, even if such a quadratic phase term is considered, it has no effect at all on the final reconstruction result.

In this experiment, the object we chose to create the image hologram was the wing of a fly. The object was positioned at a $z_s = 35$ cm distance in front of the first SLM. The other distances were set to as: $z_1 = 28$ cm and $z_2 = 92$ cm. The function displayed on the first SLM was $Q(-1/f_1)$, such that $f_1 = 27$ cm and, to form an image of the object on the CCD plane with beam B_2, the second SLM function was set to $Q(-1/f_2)$ with $f_2 = 37$ cm; thus, fulfilling the imaging condition with a magnification of

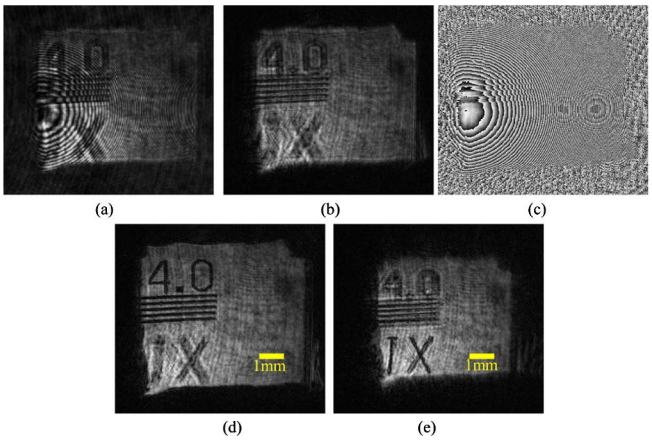

Fig. 3. Reconstruction of a three-dimensional object from its acquired Fresnel hologram. (a) Acquired Fresnel hologram for $\phi_l = 0°$. (b) Magnitude and (c) phase of the Fresnel hologram after applying the phase-shifting procedure with three exposures. (d) Reconstruction of the hologram at the best focus distance of the 4.0 object. (e) Reconstruction of the hologram at the best focus distance of the X object, which was positioned 10 cm behind the 4.0 object.

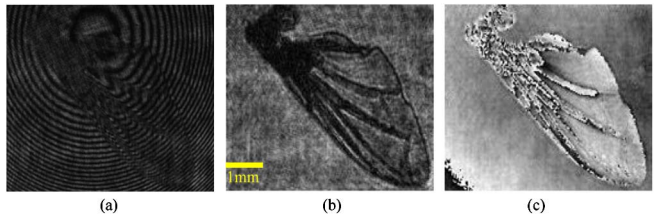

Fig. 4. Acquisition of an image hologram using JORDI. (a) Recorded hologram at $\phi_l = 0°$. (b) Amplitude and (c) phase (wrapped) of the recorded object, after the application of the phase-shifting procedure.

$M = -1.46$. The phase-shifting procedure was applied as in the first experiment. The recorded hologram with $\phi_l = 0°$ is shown in Fig. 4(a). The resultant reconstruction's magnitude and (wrapped) phase, after applying the phase-shifting procedure, and after removing from the complex hologram the linear and the quadratic phase terms, are shown in Figs. 4(b) and 4(c), respectively.

In the third experiment, we show that, by introducing a proper linear phase function on the SLMs, we are able to record a single channel, off-axis Fresnel hologram. The off-axis holography is made possible by the fact that the $L[\vec{s}]$ function on the SLMs promotes a tilt between the object and the reference wavefronts. Thus, the recording of this hologram enables the extraction of the complex field amplitude in a single shot. To demonstrate this, we have used the same setup as in the first experiment, only that this time the object was a two-dimensional resolution chart positioned at $z_s = 35$ cm. In addition, we set the linear phase function on the first SLM to be $L[\vec{a}_1/f_1]$, such that $\vec{a}_1 = (0.48\text{ cm}, 0)$. Since $f_1 = 20$ cm, this yields a tilt angle of approximately 1.4° between the object and reference beams. The acquired off-axis hologram is shown in Fig. 5(a). The magnitude of the plane of focus of the +1 order is shown in Fig. 5(b), indicating the separation between the ±1 orders. The object reconstruction from the single acquired hologram, using numerical Fresnel back-propagation, is shown in Fig. 5(c).

In the final experiment we demonstrate the advantages of the proposed setup over standard single channel, in-line, Gabor-like, holographic recording. We have recorded a Fresnel hologram using the JORDI configuration, where the fly's wing was positioned at a $z_s = 35$ cm distance in front of the first SLM. The other distances were set to $z_1 = 28$ cm and $z_2 = 92$ cm. The function displayed on the first SLM was $Q(-1/f_1)$, with $f_1 = 27$ cm.

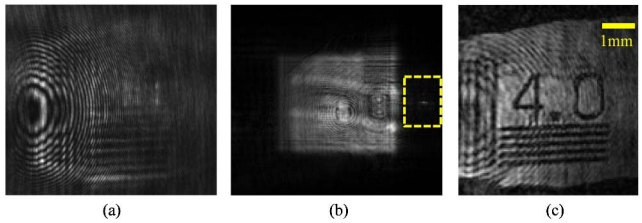

Fig. 5. Single channel off-axis holography using JORDI. (a) The recorded off-axis hologram. (b) The magnitude of the hologram at the plane in which the +1 order is focused. The reconstructed object's spectrum (+1 order) is highlighted by a dashed square, while the zero and −1 orders are out of focus. (c) Object reconstruction at best plane of focus.

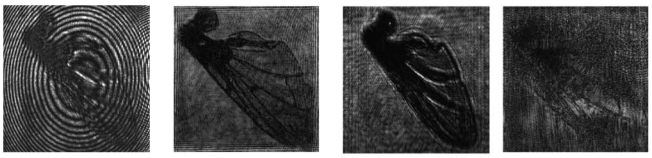

Fig. 6. Comparison of JORDI and Gabor for the fly's wing. (a), (c) The recorded JORDI and Gabor Fresnel holograms, respectively. (b), (d) The corresponding reconstructions in the best plane of focus of (a) and (c), respectively.

A Fresnel hologram was formed by setting the second SLM function to $Q(-1/f_2)$ with $f_2 = 38$ cm. The recorded hologram with $\phi_l = 0°$ is shown in Fig. 6(a). Again, the complex field amplitude at the CCD plane was extracted using the phase-shifting procedure. The reconstructed image in the best plane of focus is shown in Fig. 6(b). Then, by setting the second SLM to act like a mirror, we formed a traditional in-line Gabor hologram on the CCD. The recorded hologram is shown in Fig. 6(c), while the best focus image is shown in Fig. 6(d). On examination, the fringes in Fig. 6(c) are much weaker than those in Fig. 6(a) and, therefore, the reconstructed image in Fig. 6(d) is almost unrecognizable. This poor result of Fig. 6(d) is an indication that the nonscattered wave from the fly wing itself is too weak to be used as a reference for the Gabor hologram. Comparing the results shows a clear advantage of the proposed method in scattering samples.

In conclusion, we have proposed and demonstrated a new method to record digital holograms. While still maintaining a single channel configuration, we have recorded Fresnel and image holograms, and apply phase-shifting and off-axis holography encoding. In the proposed setup, the reference to object beam intensity ratio can be controlled easily by slightly rotating one of the polarizers from the state of equal beam division (45°); thus, the weak scattering condition is eliminated, allowing holographic recording of scattering samples. This is achieved by the ability of JORDI to provide independent control of the object and reference beams, while maintaining a single channel setup. As a single channel (in-line) configuration, which fundamentally provides high stability and space-bandwidth-product, we believe that this setup will prove suitable for microscopy and nanoscopy applications.

This work was supported by the Israel Ministry of Science and Technology (MOST) and by the Israel Science Foundation (ISF).

†Both authors contributed equally to this work.

References

1. T. Kreis, *Handbook of Holographic Interferometry: Optical and Digital Methods* (Wiley-VCH, 2005).
2. D. Gabor, Nature **161**, 777 (1948).
3. J. Rosen and G. Brooker, Opt. Lett. **32**, 912 (2007).
4. L. Xu, X. Peng, Z. Guo, J. Miao, and A. Asundi, Opt. Express **13**, 2444 (2005).
5. T. Latychevskaia and H.-W. Fink, Phys. Rev. Lett. **98**, 233901 (2007).
6. D. J. Brady, K. Choi, D. L. Marks, R. Horisaki, and S. Lim, Opt. Express **17**, 13040 (2009).
7. R. Kelner and J. Rosen, Opt. Lett. **37**, 3723 (2012).
8. V. Mico, J. Garcia, Z. Zalevsky, and B. Javidi, Opt. Lett. **34**, 1492 (2009).
9. G. Brooker, N. Siegel, V. Wang, and J. Rosen, Opt. Express **19**, 5047 (2011).
10. B. Katz and J. Rosen, Opt. Express **18**, 962 (2010).
11. J. W. Goodman, *Introduction to Fourier Optics*, 3rd ed. (Roberts & Company, 2005), Chap. 5, p. 111.